



A Meta-structure for Low-frequency Acoustic Treatment Based on a KDamper-Inertial Amplification Concept

Moris Kalderon ¹, Andreas Paradeisiotis ¹, Ioannis Antoniadis ¹

¹ Dynamics and Structures Laboratory, School of Mechanical Engineering, National Technical University of Athens, Athens, Greece.

moriska@mail.ntua.gr; aparadis@mail.ntua.gr; antogian@central.ntua.gr

Abstract

Sound transmission in passive acoustic treatment at low frequencies, is mainly controlled by two physical mechanisms: The inertial, as stated by the mass density law, and the local resonances of the structure. Consequently, conventional means for noise insulation present severe limitations in this range as the improvement of their acoustic performance is associated with the addition of extra mass. Additionally, such flexible structures have many lightly damped vibration modes at low frequencies, further hindering their effectiveness. Locally resonant acoustic meta-materials may also require the use of significant added masses, while demonstrating narrow bandgaps. This work proposes the utilization of a hybrid concept based on the optimal combination of the KDamper (KD) and Inertial Amplification mechanisms (IAM). The combined action of the negative stiffness element and the inertial amplification effect may provide extreme attenuation properties even at very low frequencies. The theoretical framework for a meta-structure based on the periodic repetition of KD-IAM unit cells is established. It is shown to generate deep and wide attenuation bands in the region of the fundamental resonance of the structure, surpassing the mass density law while utilizing a fraction of the additional mass of comparable concepts. An indicative implementation of the meta-structure is also presented and validated via Finite Element Analysis.

Keywords: KDamper, Inertia Amplification, Metamaterial, Design, low frequency.

1 Introduction

The term “acoustic meta-materials” [1] describes periodic structures with unit cells exhibiting local resonance. The base of such designs is described by a simple “mass-in-mass” lumped parameter model, resulting in negative effective stiffness or mass at frequency ranges close to the local resonances. This localized resonant structure exhibit band-gaps at wavelengths much longer than the lattice size [2–5], thus enabling low-frequency vibration attenuation, wave guiding, and filtering, among other applications.

However, low frequency range applications of such locally resonant meta-materials, may require very heavy internal moving masses, as well as additional constraints at the amplitudes of the internally oscillating locally resonating structures, which may prohibit their practical implementation. For example, current applications of locally resonant meta-materials in acoustics [6,7] often address frequencies well above 500 [Hz]. Additionally, it should be mentioned that conventional acoustic panels perform poorly in this frequency range, thus, there is an all increasing trend towards the design of a new generation of structures with increased isolation properties in the low-frequency regime.

To contribute to the solution of low frequency sound attenuation, the current research considers the application of an enhanced KDamping concept [8] incorporating an inertial amplification mechanism (IAM) for the design of highly dissipative low-frequency acoustic meta-materials. The KDamper [9,10] is a novel passive vibration

isolation and damping concept, based essentially on the optimal combination of appropriate stiffness elements, which include a negative stiffness element. The KDamper (KD) can be considered as an extension of the traditional Tuned Mass Damper (TMD), by the addition of a negative stiffness element to the internal oscillating mass. On the other hand, the concept of inertial amplification goes back many decades [11]. Hence, inspired by their successful application in engineering concepts [12,13], several works used the similar concept of inertial amplification mechanisms (IAMs) for the formation of finite periodic structures and bandgap generation. The fundamental theory regarding the generation of phononic gaps utilizing IAMs [14] has been tested by a first design with flexural hinges which was experimentally validated [15]. The effectiveness and characteristics of the IAM concept can also be utilized in low-frequency noise insulation. As proposed in this work, in combination with the properties of the KDamper, the width and depth of the generated low-frequency attenuation band can be further improved. An extended KDamper framework that incorporates an IAM is thus presented. This coupled absorber is applied to form a novel periodic structure, resulting in a wide and deep frequency band of improved vibration and noise attenuation.

The present contribution is structured as follows: First, the KD-IAM concept is described and then based on Bloch's theorem the one-dimensional mass-in-mass lattice is analysed and the corresponding dispersion relations are derived. Next, utilizing the lumped parameter model (LPM) [16] as a convenient and fast approximative method we evaluate the STL in this region based on a couple of transfer functions, where distinction is made between localized masses and masses corresponding to radiating surfaces. Exploiting this theory, we present initial designs of the corresponding parts and finally, we assess the performance of the KD-IAM meta-structure through a detailed Finite element vibro-acoustic model.

2 KDamper-IAM Meta-material

2.1 Overview of the KDamper-IAM Concept

Figure 1 presents the basic layout of the KD-IAM concept. The KDamper theoretical framework [17] is extended to include the case where the rigid mass is replaced by a deformable plate, where m_1 is the modal mass of the panel and k_1 the bending stiffness. In order to do that, the main assumption is that the bending stiffness of the deformable plate is in a way in series with the stiffness of the KD-IAM. Moreover, since the loss factor (n) can represent more accurately the dynamic response of nonlinear systems compared with the damping ratio which is defined on the grounds of the linear single degree of freedom (SDOF) viscous model [18], hysteretic damping is introduced indirectly considering complex stiffness elements as

$$k'_s = k_s(1 + jn) \quad (1)$$

$$k'_p = k_p(1 + jn) \quad (2)$$

The corresponding model is realized based on the KDamper with the inclusion of the inertial amplifier (IAM), where m_j is the connecting mass which is assumed as negligible in order to act just as a connector, namely an additional DOF. The effective mass of the IAM is calculated as [13]:

$$m_B = \frac{m_a}{2} [\cot^2 \theta + 1] \quad (3)$$

The equations of motion resulting from the model of the panel mounted in KDamper mounts come as

$$m_1 \ddot{q}_1 + k_1(q_1 - q_2) = F \quad (4)$$

$$m_B \ddot{q}_2 - k^* q_1 + (k^* + k'_p + k'_s) q_2 - k'_p q_3 = 0 \quad (5)$$

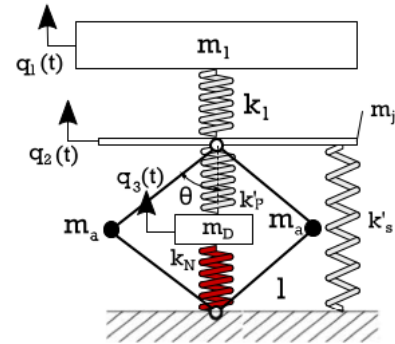


Figure 1 – Basic layout of the KD-IAM concept where the mechanism supports a deformable plate.

$$m_D \ddot{q}_3 + (k'_p + k'_s)q_3 - k'_p q_2 = 0 \quad (6)$$

2.2 Dispersion Relations and Equation of Motion

The KD-IAM [16] unit cell is depicted in Figure 2 for the simplest case of a meta-structure based on the periodic repetition of such unit cells. The periodicity is considered one dimensional, and the IAMs are grounded on one end.

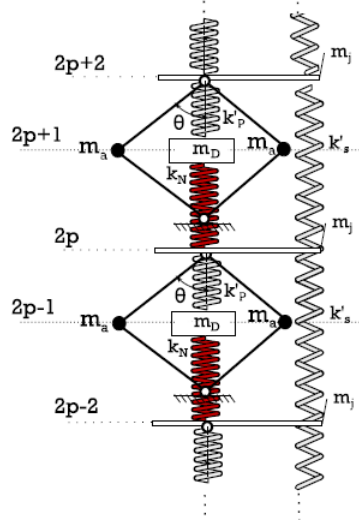


Figure 2 – KD-IAM unit cell.

The displacement of a DoF at a certain position $2p$ of the lattice may be expressed in a complex notation as.

$$u_{2p} = \tilde{u}_{2p} e^{\sigma t} = U(2p\kappa L) e^{j2p\kappa L}, \quad (7)$$

with κ being the wavenumber and L being the length of the unit cell. In the time part of the solution, the parameter σ is defined as $\sigma = \pm j\Omega$, or in the case where the attenuation between the unit cells is considered,

$$\sigma = -\zeta(\kappa)\Omega(\kappa) \pm j\omega_n \sqrt{1 - \zeta^2(\kappa)}, \text{ where } \zeta \text{ is the damping ratio.}$$

Utilizing Bloch's theory, the propagation of elastic waves between unit cells can be described by considering the interaction of displacements and forces. Considering the spatial part of the solution, this is expressed as

$$u_{2p} = U e^{j2p\kappa L}, \quad (8)$$

$$u_{2p-2} = u_{2p} e^{-j2\kappa L}, \quad (9)$$

$$u_{2p+2} = u_{2p} e^{j2\kappa L}, \quad (10)$$

$$u_{2p-1} = U_D e^{j2p\kappa L} e^{-j\kappa L}, \quad (11)$$

$$u_{2p+1} = u_{2p-1} e^{j2\kappa L}. \quad (12)$$

Assuming the case without damping, substitution into the equations of motion of the unit cell leads to

$$m_B m_D \Omega^4 - [m_B k_D + (\gamma k_S + k_D) m_D] \Omega^2 + \gamma (k_S k_D + k_P k_N) = 0 \quad (13)$$

where $\gamma = 2(1 - \cos q)$ for $q = 2\kappa L$ and $k_D = k_P + k_N$. Setting $\lambda = \Omega^2$, Eq. (13) can be written as

$$A\lambda^2 + B\lambda + C = 0, \quad (14)$$

where

$$A = 1, B = -[(1 + \mu_B)\omega_D^2 + \gamma\omega_{S,B}^2], C = \gamma\omega_B^2\omega_D^2, \quad (15)$$

having defined the following characteristic frequencies and parameters:

$$\omega_B = \sqrt{k_0/m_B}, \omega_{S,B} = \sqrt{k_S/m_B}, \mu_B = \sqrt{m_D/m_B} \quad (16)$$

Then, the dispersion relations are given by the two solutions λ_1, λ_2 of Eq. (14), resulting in the upper $\omega^+(q) = \sqrt{\lambda_1}$ and lower $\omega^-(q) = \sqrt{\lambda_2}$ branches, respectively.

The dispersion relations are $2\pi/L$ -periodic in the wavenumber space; therefore, $\omega(q) = \omega(q + 2\pi)$. Furthermore, considering the irreducible Brillouin zone, the two characteristic high (ω_H) and low (ω_L) frequencies of the generated bandgap can be calculated as

$$\omega_H = \omega^+(q = 0) = \omega_D\sqrt{1 + \mu_B} = \omega_B\rho_B\sqrt{1 + \mu_B} \quad (17)$$

$$\omega_L = \omega^-(q = \pi) = \frac{1}{\sqrt{2}}\sqrt{4\omega_{S,B}^2 + \omega_H^2 - \sqrt{(4\omega_{S,B}^2 + \omega_H^2)^2 - (4\omega_B\omega_D)^2}} \quad (18)$$

where $\kappa_D = k_D/k_0$. The above frequencies can be used for tuning of the meta-structure for a specific application and for the definition of the normalized bandgap width in the form

$$b_w = (f_H - f_L)/f_{av}, \quad (19)$$

where $f_{av} = (f_H + f_L)/2$.

Concerning the equation of motion of the meta-material, for M number of unit cells is expressed in matrix formulation as

$$\mathbf{M} \ddot{\mathbf{u}}(t) + \mathbf{K} \mathbf{u}(t) = \mathbf{F} \mathbf{f}(t) \quad (20)$$

where $\mathbf{M}_{n \times n}$, $\mathbf{K}_{n \times n}$, $\dot{\mathbf{u}}_{n \times 1}$, $\mathbf{u}_{n \times 1}$, $\mathbf{u}_{n \times 1}$, $\mathbf{F}_{n \times 1}$ and $n = 2M + 3$ is the number of degrees of freedom of the meta-material. Indicatively, for a single unit cell, M=1, the mass [\mathbf{M}], and stiffness [\mathbf{K}] matrices come as

$$\mathbf{M} = \begin{bmatrix} m^* & 0 & 0 & 0 & 0 \\ 0 & m_B & 0 & 0 & 0 \\ 0 & 0 & m_D & 0 & 0 \\ 0 & 0 & 0 & m_B & 0 \\ 0 & 0 & 0 & 0 & m^* \end{bmatrix} \quad (21)$$

$$\mathbf{K} = \begin{bmatrix} k^* & -k^* & 0 & 0 & 0 \\ -k^* & k_S + k_p + k^* & -k_p & -k_S & 0 \\ 0 & -k_p & k_p + k_N & -k_N & 0 \\ 0 & -k_S & -k_N & k_S + k_N + k^* & -k^* \\ 0 & 0 & 0 & -k^* & k^* \end{bmatrix}, \quad \mathbf{F} = \begin{bmatrix} 1 \\ 0 \\ 0 \\ 0 \\ 0 \end{bmatrix}$$

For $M > 1$, the above matrices of the single unit cell, are added appropriately. Therefore, the transfer functions of each degree of freedom to the excitation may be calculated via the following expression,

$$\mathbf{TF} = (-\Omega^2 \mathbf{M} + \mathbf{K})^{-1} \mathbf{F} \quad (22)$$

In order to formulate a more realistic sandwich-type meta-structure the previously defined modal mass of the panel m_1 is divided in two masses enclosing the periodic chain in both ends. This modelling technique is required to simulate the effect of the radiating surface and the consequent calculation of the STL [16]. The STL of the KDamper model is then calculated as $STL_{KD} = 10 \log_{10}(\frac{1}{\tau_{kD}})$ and the transmission coefficient

τ_{KD} is given as

$$\tau_{KD} = l_x l_y \left(\frac{4\Omega^2 \rho_0}{\pi^3} \right)^2 \frac{1}{|(-\Omega^2 m^* + k^*)(1 - TF_{21})|^2} I_{\theta, \phi} \quad (23)$$

Where, l_x, l_y are the dimensions of the radiating surfaces, ρ_0 the air density, $I_{\theta, \phi}$ the integral over hemispheric surface and $TF_{21} = \mathbf{TF}(2)/\mathbf{TF}(1)$.

2.3 Case study

In this section, an examination of the KD-IAM concept is presented, considering the low-frequency acoustic performance of the meta-structure. The values of the KD-IAM parameters are tabulated in Table 1 and are obtained after an optimization procedure. Relevant information about the optimization procedure can be found in [16]. The panels enclosing the periodic KD-IAM structure are assumed to be comprised by conventional plasterboards, the properties of which are summarized in Table 2.

Table 1 – Values of the optimized KD-IAM parameters.

f_1 [Hz]	f_{KD}	k_0 [N/mm]	k_S [N/mm]	k_P [N/mm]	k_N [N/mm]	μ	η	κ_N	m_B [kg]
100	25.1	140.5	412.1	158.1	-102	0.01	0.1	-0.679	3.49

Table 2 – Plasterboard properties.

ρ_p [kg/m ³]	l_x [m]	l_y [m]	h_p [mm]	E_p [MPa]	ν_p	η_p
668	1.2	2.4	6.3	2900	0.31	0.01

Figure 3 (a) depicts the bandgap frequencies of the irreducible Brillouin zone for the selected geometry and parameters where $f_H = 163.32$ Hz and $f_L = 56.67$ Hz, corresponding to a normalized bandgap width $b_w = 1.89$. Accordingly, Figure 3 (b) demonstrates the acoustic performance of the sandwich panel based on the periodic repetition of KD-IAM unit cells.

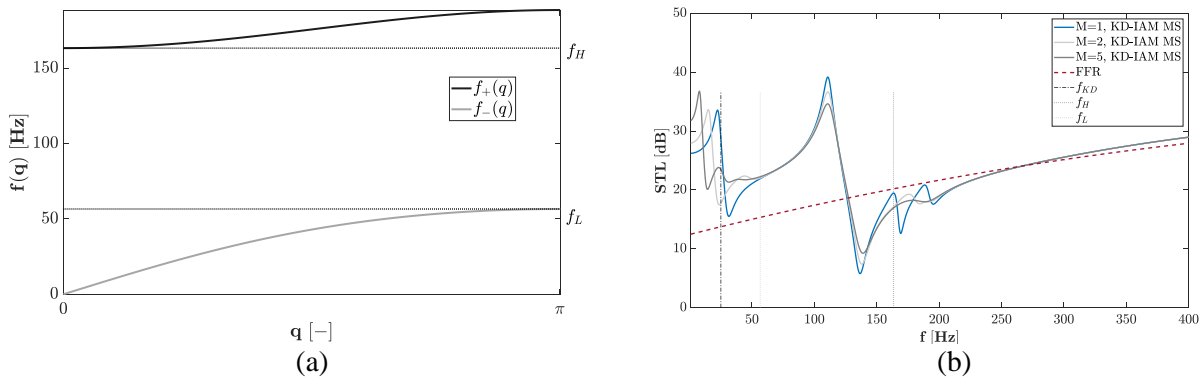


Figure 3 – Performance of the KD-IAM periodic structure. (a) Dispersion curves: irreducible Brillouin zone. (b) STL for various numbers M of unit cells.

The depth and width of the attenuation band are not significantly affected as far as the STL performance is concerned. However, despite the choice of lower loss factor, the emergence of meta-damping improves the response around the characteristic frequency f_0 , which can be very important for certain applications. However, in the context of the present investigation, it is demonstrated that the physical mechanisms of the KD-IAM concept providing this extreme attenuation band are present even for a single unit cell, meaning that, at least in this specific case, the added manufacturing complexity for multiple unit cells could be deemed unnecessary.

3 Indicative KD-IAM Metastructure design

Figure 4 shows a feasible conceptual design for such a meta structure for $M=1$ number of unit cells. Naturally, the various parallel KD-IAM elements can be divided according to the number of positions and such unit cells are chosen to be positioned on the surfaces of the panels. The rationale behind the quantity of each element lies on the required properties that should be realized, the constraints that apply due to their dimensions and the requirement of an adequate number of supports in order to achieve a uniform pressure distribution on the surface of each panel. Specifically, sixteen (16) negative stiffness elements are utilized, eight (8) at each panel, and two (2) k_p springs are located on top of each negative spring. Concerning the k_s springs, a total number of thirty two (32) elements is prescribed divided again accordingly to the two panels. Lastly, fifty-four (54) IAMs are considered in total in order to achieve the required amplification.

The positive springs (k_s and k_p) are envisaged to be made of acrylonitrile butadiene styrene (ABS), a material that can be used in conventional 3D printers. On the other hand, the negative stiffness springs and the amplifiers are made of steel. The ABS material is modelled as linear elastic-perfectly plastic, with Young's modulus, $E=1740$ MPa, yield stress $\sigma_{yield}=27.8$ MPa and mass density, $\rho=1100$ kg/m³ and steel is modelled as linear elastic-perfectly plastic, with Young's modulus, $E=210$ GPa, yield stress $\sigma_{yield}=275$ MPa and mass density, $\rho=7800$ kg/m³.



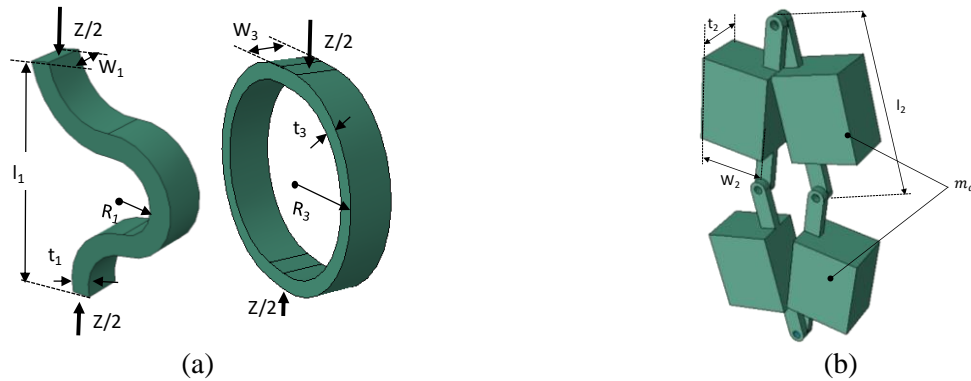
Figure 4 – KD-IAM meta-structure conceptual design.

To enable simple fabrication in a single material system without the need for complex assembly, the positive springs are implemented as arches. The shapes of the semicircular arches implementing the springs k_s and k_p are chosen to allow large strains in the linear regime without yielding or buckling. Clearly, this poses a limit on the stiffness of the entire system, as both springs are bending-dominated. The widths and thicknesses of all the elements are properly adjusted to result in the desired stiffness, which was initially calculated based on Eq. (24) and (25) [19].

$$k_p = 1.38 E w_1 \left(\frac{t_1}{l_1} \right)^3 \quad (24)$$

$$k_s = 0.46 E w_3 \left(\frac{t_3}{R_3} \right)^3 \quad (25)$$

The geometry of the positive springs is depicted in Figure 5 (a) and the relevant geometrical parameters are gathered in Table 3.



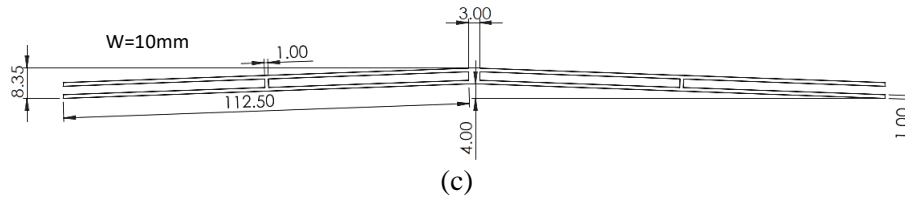


Figure 5 – Geometry of the (a) k_s and k_p springs, (b) of the IAM, (c) of the k_N springs.

In order to verify the simple analytical models, Finite Elements (FE) simulation is conducted with the commercial software ABAQUS®. The springs are modeled with solid elements and a Rik's post-buckling analysis is performed. The load-displacement curves for these springs are presented in Figure 6 (a) and (b), together with the results of the FE predictions. In both cases it is observed that springs behave linearly elastic for deformation less than 3mm, which is deemed as adequate.

Table 3– Positive springs parameters.

Spring	t [mm]	R [mm]	w [mm]	l [mm]	Stiffness / spring [N/m]	Number of springs / panel	Stiffness / panel [N/m]
k_s	3	20	9	40	$2.4 \cdot 10^4$	16	$4.32 \cdot 10^5$
k_p	3	8	5	32	$9.9 \cdot 10^3$	16	$1.58 \cdot 10^5$

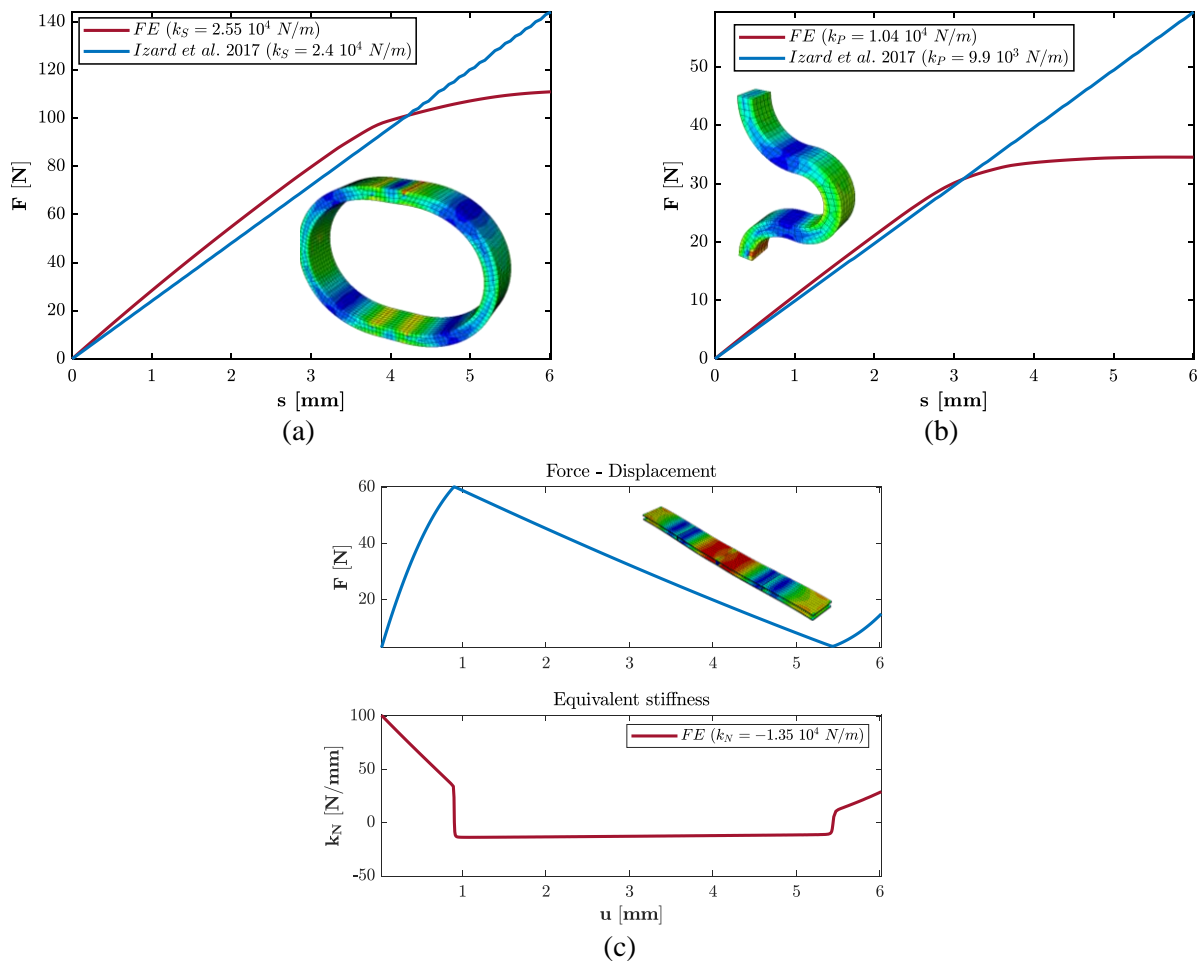


Figure 6 – Load – displacement curves of the springs (a) k_s (b) k_p (c) k_N .

In this implementation, the negative stiffness element is realized utilizing inclined pre-stressed beams. The dimensions of the selected beams are depicted in Figure 5 (c) where three (3) ABS spacers connect the two (2) steel blades and urge the beams to buckle at the required locations. Again, FE Rik's analysis is performed to capture the snap-through behaviour and the load-displacement curves are obtained according to Figure 6 (c). The range of the vertical displacement s where the disk exhibits the desired negative stiffness characteristics is centered around the flat position of the beam where the exerted force and the stiffness attains its maximum negative value. In order to achieve the required negative stiffness value, with the geometrical properties presented, eight (8) springs with $k_N/8 = -1.35 \times 10^4 \text{ N/m}$ have to be configured.

As given in Eq. (3), the mass m_a of the IAM has an amplification factor $(\cot^2 \theta + 1)$. Therefore, for realization of the IAM a combination of (m_a, θ) needs to be selected in order to provide the desired m_B . For this particular design, assuming structural steel for the material of the IAM and hinged connections as shown in Figure 5(b), the relevant parameters for the IAM mechanism are summarized in Table 4.

Table 4 – IAM mechanism parameters.

l_2 [mm]	t_2 (mm)	w_2 (mm)	m_a (kg) / IAM	Number of IAMs / panel	Amplified mass / panel
20	6	10	0.0156	27	0.42

4 Performance of the KDamper-IAM meta-structure

Finally, the performance of the sandwich meta-panel is assessed through a detailed Finite element vibro-acoustic model. As a simplification only the transmission side of the air domain is modeled and the panel is excited by directly applying the blocked pressure ($p_b = 2p_i$) on its surface, see Figure 7. The acoustic pressure is extracted from the fluid-structure interface nodes and then the arithmetic average is calculated as

$$\bar{P}_t = \frac{1}{n} \sum_{i=1}^n |p_{t,i}| \quad (26)$$

where n denotes the total number of nodes; i denotes the node number; and p_t denotes the transmitted pressure. Then the averaged pressure was used to compute the simulated STL by

$$STL = 20 \log_{10} \frac{|P_i|}{\bar{P}_t} \quad (27)$$

The panel is discretized by 20-node quadratic solid hexahedral elements and the fluid domain is discretized by 20-node quadratic acoustic hexahedral elements. The springs and the amplifiers are modeled based on the design described in the previous section. Tie constraints are used to simulate the coupling of the fluid-structure interface and non-reflecting boundary conditions are specified to generate the infinite fluid domain. Lastly, the discretization of the fluid domain has more than three quadratic elements across the minimum wavelength of interest to increase the accuracy of the computational results [20].

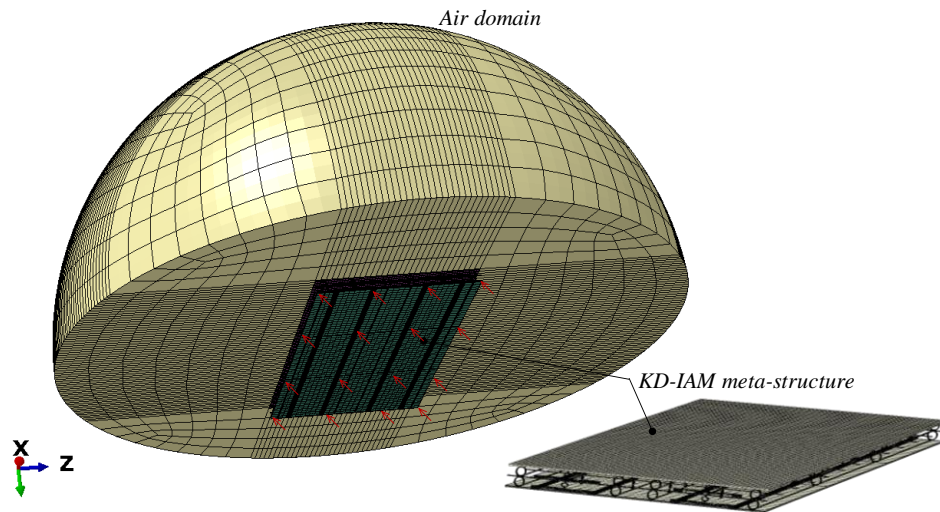


Figure 7 – KD-IAM meta-structure Finite Element model.

Figure 8 presents the results of the FE simulation of the KD-IAM meta-structure with one unit cell. Obviously, in reality the acoustic performance of such a meta-structure is much more complex and difficult to be predicted exactly. The main reason is the positioning of the various structural elements between the panels. Depending on the chosen configuration, the dynamic response may vary significantly. In this particular case, the frequency range of improved STL is slightly higher than what was predicted analytically, specifically between 120 and 220 Hz, compared to the free finite rigid (FFR) panel approximation.

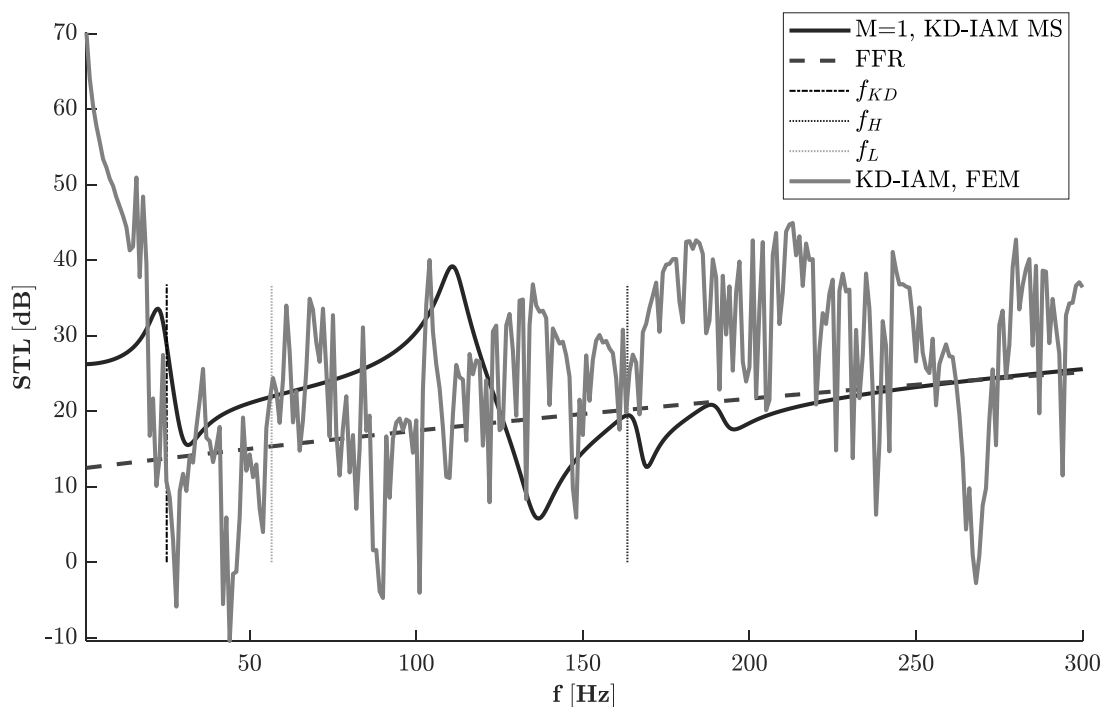


Figure 8 – STL Performance of the KD-IAM meta structure.

In any case, the lumped parameter models of the acoustic meta-structure provide a reasonable approach for the dimensioning of the various elements and an estimation of the expected performance. Additionally, a more

refined FE model can provide further insight of the real performance and the effect of the positioning configuration of the stiffness elements.

5 Conclusions

In this paper, the vibration and sound properties of a sandwich meta-structure are presented. The proposed metamaterial is essentially based on the synergetic KDamping and Inertial amplification concepts. First the theoretical framework of the periodic structure is presented. Then, based on a typical case study in a building acoustic's application it is shown that deep and wide bandgaps can be formed in the low-frequency regime. Thus, the KD-IAM is deemed extremely capable for low frequency acoustic insulation without the requirement of many unit cells and the added complexity that could be entailed in a practical implementation. Finally, the feasibility of the concept is demonstrated by providing preliminary designs of all the essential parts comprising the KD-IAM meta-structure. Appropriate technological implementations of this concept can lead to significant improvements in all types of low-frequency technological applications, with emphasis in low-frequency noise isolation-absorption.

Acknowledgements

Moris Kalderon has been financed by the European Union's Horizon 2020 research and innovation programme under the Marie Skłodowska-Curie grant (Grant Agreement No. INSPIRE-813424, "INSPIRE—Innovative Ground Interface Concepts for Structure Protection").

References

- [1] Hussein, M.I.; Leamy, M.J.; Ruzzene, M. Dynamics of Phononic Materials and Structures: Historical Origins, Recent Progress, and Future Outlook. *Applied Mechanics Reviews* 2014, Vol 66, doi:10.1115/1.4026911.
- [2] Liu, Z.; Zhang, X.; Mao, Y.; Zhu, Y.Y.; Yang, Z.; Chan, C.T.; Sheng, P. Locally Resonant Sonic Materials. *Science* 2000, Vol 289, 1734–1736, doi:10.1126/science.289.5485.1734.
- [3] Li, J.; Chan, C.T. Double-Negative Acoustic Metamaterial. *Phys. Rev. E* 2004, Vol 70, 55602, doi:10.1103/PhysRevE.70.055602.
- [4] Chen, Y.; Huang, G.; Zhou, X.; Hu, G.; Sun, C.-T. Analytical Coupled Vibroacoustic Modeling of Membrane-Type Acoustic Metamaterials: Plate Model. *The Journal of the Acoustical Society of America* 2014, Vol 136, 2926–2934.
- [5] Huang, H.H.; Sun, C.T.; Huang, G.L. On the Negative Effective Mass Density in Acoustic Metamaterials. *International Journal of Engineering Science* 2009, Vol 47, 610–617, doi:https://doi.org/10.1016/j.ijengsci.2008.12.007.
- [6] Groby, J.-P.; Lagarrigue, C.; Brouard, B.; Dazel, O.; Tournat, V.; Nennig, B. Using Simple Shape Three-Dimensional Rigid Inclusions to Enhance Porous Layer Absorption. *The Journal of the Acoustical Society of America* 2014, Vol 136, 1139–1148.
- [7] Weisser, T.; Schwan, L.; Groby, J.-P.; Lagarrigue, C.; Deckers, E.; Dazel, O. Poroelastic Subwavelength Absorber with Both Elastic and Acoustic Embedded Resonator. In Proceedings of the Proceedings of the 27th International Conference on Noise and Vibration Engineering; 2016; pp. 2127–2136.
- [8] Antoniadis, I.A.; Paradeisiotis, A. Acoustic Meta-Materials Incorporating the KDamper Concept for Low Frequency Acoustic Isolation. *Acta Acustica united with Acustica* 2018, Vol 104, 636–646.

- [9] Antoniadis, I.; Chronopoulos, D.; Spitas, V.; Koulocheris, D. Hyper-Damping Properties of a Stiff and Stable Linear Oscillator with a Negative Stiffness Element. *Journal of Sound and Vibration* 2015, Vol 346, 37–52, doi:<https://doi.org/10.1016/j.jsv.2015.02.028>.
- [10] Paradeisiotis, A.; Kalderon, M.; Antoniadis, I.; Fouriki, L. Acoustic Performance Evaluation of a Panel Utilizing Negative Stiffness Mounting for Low Frequency Noise Control. In Proceedings of the Proceedings of EURO DYN 2020; EASD Procedia: Athens, Greece, 23–26 November, 2020; pp. 4093–4110.
- [11] Flannelly, W.G. Best Invention Ever 1967.
- [12] Kalderon, M.; Paradeisiotis, A.; Antoniadis, I. 2D Dynamic Directional Amplification (DDA) in Phononic Metamaterials. *Materials* 2021, Vol 14, doi:[10.3390/ma14092302](https://doi.org/10.3390/ma14092302).
- [13] Cheng, Z.; Palermo, A.; Shi, Z.; Marzani, A. Enhanced Tuned Mass Damper Using an Inertial Amplification Mechanism. *Journal of Sound and Vibration* 2020, Vol 475, 115267.
- [14] Yilmaz, C.; Hulbert, G.M. Theory of Phononic Gaps Induced by Inertial Amplification in Finite Structures. *Physics Letters, Section A: General, Atomic and Solid State Physics* 2010, Vol 374, 3576–3584.
- [15] Acar, G.; Yilmaz, C. Experimental and Numerical Evidence for the Existence of Wide and Deep Phononic Gaps Induced by Inertial Amplification in Two-Dimensional Solid Structures. *Journal of Sound and Vibration* 2013, Vol 332, 6389–6404.
- [16] Paradeisiotis, A.; Kalderon, M.; Antoniadis, I. Advanced Negative Stiffness Absorber for Low-Frequency Noise Insulation of Panels. *AIP Advances* 2021, Vol 11, 65003, doi:[10.1063/5.0045937](https://doi.org/10.1063/5.0045937).
- [17] Paradeisiotis, A.; Antoniadis, I. Implementation of a Low Frequency Acoustic Isolation Panel Incorporating KDamper Based Mounts. In Proceedings of the Proceedings of ICOVP 2019; Crete, Greece, 2019.
- [18] Carfagni, M.; Lenzi, E.; Pierini, M. The Loss Factor as a Measure of Mechanical Damping. 1998, 580.
- [19] Guell Izard, A.; Fabian Alfonso, R.; McKnight, G.; Valdevit, L. Optimal Design of a Cellular Material Encompassing Negative Stiffness Elements for Unique Combinations of Stiffness and Elastic Hysteresis. *Materials & Design* 2017, Vol 135, 37–50, doi:<https://doi.org/10.1016/j.matdes.2017.09.001>.
- [20] Marburg, S. Six Boundary Elements per Wavelength: Is That Enough? *Journal of Computational Acoustics* 2002, Vol 10, 25–51.